J|A|C|S
ARTICLES
Published on Web 10/26/2006

High-Performance Air-Stable n-Type Transistors with an Asymmetrical Device Configuration Based on Organic Single-Crystalline Submicrometer/Nanometer Ribbons

Qingxin Tang,[†,‡] Hongxiang Li,*[,†] Yaling Liu,[†,‡] and Wenping Hu*[,†]

Contribution from the Beijing National Laboratory for Molecular Sciences, Key Laboratory of Organic Solids, Institute of Chemistry, Chinese Academy of Sciences, Beijing 100080, and Graduate School of the Chinese Academy of Sciences, Beijing 100039, People's Republic of China

Received July 6, 2006; E-mail: huwp@iccas.ac.cn

Abstract: High-performance air-stable n-type field-effect transistors based on single-crystalline submicro- and nanometer ribbons of copper hexadecafluorophthalocyanine (F_{16}CuPc) were studied by using a novel device configuration. These submicro- and nanometer ribbons were synthesized by a physical vapor transport technique and characterized by the powder X-ray diffraction pattern and selected area electron diffraction pattern of transmission electron microscopy. They were found to crystallize in a structure different from that of copper phthalocyanine. These single-crystalline submicro- and nanometer ribbons could be in situ grown along the surface of Si/SiO_2 substrates during synthesis. The intimate contact between the crystal and the insulator surface generated by the "in situ growing process" was free from the general disadvantages of the handpicking process for the fabrication of organic single-crystal devices. High performance was observed in devices with an asymmetrical drain/source (Au/Ag) electrode configuration because in such devices a stepwise energy level between the electrodes and the lowest unoccupied molecular orbital of F_{16}CuPc was built, which was beneficial to electron injection and transport. The field-effect mobility of such devices was calculated to be $\sim$0.2 $cm^2\ V^{-1}\ s^{-1}$ with the on/off ratio at $\sim 6 \times 10^4$. The performances of the transistors were air stable and highly reproducible.

Introduction

n-type semiconductors have been widely applied in inorganic electronics, especially in digital circuits, to work as complementary circuits which effectively lower power dissipation, improve noise immunity, and increase operational stability.[1] However, for organic electronics, a few n-type semiconductors and their field-effect transistors, especially air-stable ones, have been investigated. The synthesis of n-type semiconductors is difficult, and most n-type organic semiconductors are air sensitive. Moreover, in the commonly used symmetrical device configuration for n-type organic field-effect transistors (OFETs), e.g., Au/Au or Ag/Ag as the drain/source, it is difficult to match the work function of the electrode with the lowest unoccupied molecular orbital (LUMO) of organic semiconductors, resulting in the deterioration of the performance of n-type OFETs.[1]

Single crystals have prominent merits in the study of intrinsic charge-transport properties of organic semiconductors, and some single-crystal OFETs exhibit mobility higher than 1 $cm^2\ V^{-1}\ s^{-1}$,[2] which opens up prospects for the fabrication of high-quality devices and circuits.[2f] Nevertheless, there are still many factors limiting their applications. Two challenging tasks are growing large-size organic crystals and handling such fragile crystals. As we know, most organic crystals always exist on the micro- or nanometer scale. It is challenging to grow large-size organic crystals, even on the millimeter scale. Hence, if OFETs could be fabricated directly based on micro- or nanometer-scale crystals, which will not only overcome the challenge to grow large-size crystals but also keep all the advantages of organic single crystals, it will provide a direct way to characterize the intrinsic properties of organic semiconductors. Furthermore, devices on the submicro- and nanometer scales have attracted particular attention recently with the development of nanoelectronics. Though nanodevices based on carbon nanotubes[3] and inorganic semiconductors[4] have been extensively studied, only

[†] Chinese Academy of Sciences.
[‡] Graduate School of the Chinese Academy of Sciences.

(1) (a) Meijer, E. J.; Deeuw, D. M.; Setayesh, S.; Vanveenendaal, E.; Huisman, B.-H.; Blom, P. W. M.; Hummelen, J. C.; Scherf, U.; Klapwijk, T. M. *Nat. Mater.* **2003**, *2*, 678−682. (b) Crone, B.; Dodabalapur, A.; Lin, Y.-Y.; Filas, R. W.; Bao, Z.; LaDuca, A.; Sarpeshkar, R.; Katz, H. E.; Li, W. *Nature (London)* **2000**, *403*, 521−523.

(2) (a) Horowitz, G.; Bachet, B.; Yassar, A.; Lang, P.; Demanze, F.; Fave, J.-L.; Garnier, F. *Chem. Mater.* **1995**, *7*, 1337−1341. (b) Katz, H. E.; Lovinger, A. J.; Laquindanum, J. G. *Chem. Mater.* **1998**, *10*, 457−459. (c) Sundar, V. C.; Zaumseil, J.; Podzorov, V.; Menard, E.; Willett, R. L.; Someya, T.; Gershenson, M. E.; Rogers, J. A. *Science* **2004**, *303*, 1644−1646. (d) Podzorov, V.; Pudalov, V. M.; Gershenson, M. E. *Appl. Phys. Lett.* **2003**, *82*, 1739−1741. (e) Podzorov, V.; Sysoev, S. E.; Loginova, E.; Pudalov, V. M.; Gershenson, M. E. *Appl. Phys. Lett.* **2003**, *83*, 3504−3506. (f) de Boer, R. W. I.; Gershenson, M. E.; Morpurgo, A. F.; Podzorov, V. *Phys. Status Solidi A* **2004**, *201*, 1302−1331.

(3) (a) Javey, A.; Guo, J.; Wang, Q.; Lundstrom, M.; Dai, H. *Nature (London)* **2003**, *424*, 654−657. (b) Tans, S. J.; Verschueren, A. R. M.; Dekker: C. *Nature (London)* **1998**, *393*, 49−52.

10.1021/ja064476f CCC: $33.50

a small amount of literature has addressed single crystals of organic semiconductors, especially *n*-type organic semiconductors.

Copper hexadecafluorophthalocyanine (F_{16}CuPc) has attracted attention in OFETs due to its remarkable air-stable n-type semiconducting properties as well as its high thermal and chemical stability.[5] Pioneer works of Bao et al. demonstrated that the mobility of its thin-film OFETs could reach 0.03 cm^2 V^{-1} s^{-1}.[5a] It is regretful that up to date the structure of F_{16}CuPc has not been well studied (to our knowledge, its structure was only hypothesized as similar to that of copper phthalocyanine (CuPc)[5a,6]) and no single-crystal devices based on F_{16}CuPc have ever been investigated.

We acknowledge the great meaning and prospect for the study of F_{16}CuPc as well as the status of the compound encountered. First, single-crystalline submicro- and nanometer ribbons of F_{16}CuPc were synthesized by the vapor transport technique. The crystal structure of the submicro- and nanometer ribbons was investigated by X-ray powder diffraction (XRD) and selected area electron diffraction (SAED), the results of which suggested that the structure of F_{16}CuPc was different from that of CuPc. Moreover, it was found that single-crystalline submicro- and nanometer ribbons could be in situ grown on a SiO_2 surface for various architectures and device applications. High performance was observed in devices with an asymmetrical drain/source (Au/Ag) electrode configuration based on single-crystal submicro- or nanoribbons of F_{16}CuPc, because in such devices a stepwise energy level between the electrodes and the LUMO of F_{16}CuPc was built, which was beneficial to electron injection and transport. The field-effect mobility of such devices was calculated over 0.2 cm^2 V^{-1} s^{-1} with the on/off ratio at $\sim 6 \times 10^4$. The performances of the transistors were air stable and highly reproducible.

Experimental Section

F_{16}CuPc was purchased from Aldrich, and the submicro- and nanometer ribbons of F_{16}CuPc were fabricated in a two-zone horizontal tube furnace.[7] A quartz boat with F_{16}CuPc powder was placed at the high-temperature zone and vaporized at 380−450 °C. Highly pure Ar was used as the carrier gas, and the system was evacuated by a mechanical pump. Deep-blue fuzzlike products, which were found to be F_{16}CuPc ribbons later, were obtained at the low-temperature zone. F_{16}CuPc was regrown three times by using the ribbons collected from the first growth as the source material for the next growth to gain high purity. OFETs based on submicro- and nanometer ribbons of F_{16}CuPc were fabricated with a coplanar electrode geometry on Si/SiO_2 substrates. Au and Ag were deposited on an individual ribbon as drain and source electrodes by the "multiple times gold wire mask moving" technique.[8]

The morphology of the product was examined using field-emission scanning electron microscopy (SEM; Hitachi S-4300) and transmission electron microscopy (TEM; JEOL 2010). The structures were analyzed by XRD (Rigaku D/max 2500) and SAED (JEOL 2010). Current−voltage ($I-V$) characteristics of OFETs were recorded with a Keithley 4200 SCS and a Micromanipulator 6150 probe station in a clean and shielded box at room temperature in air.

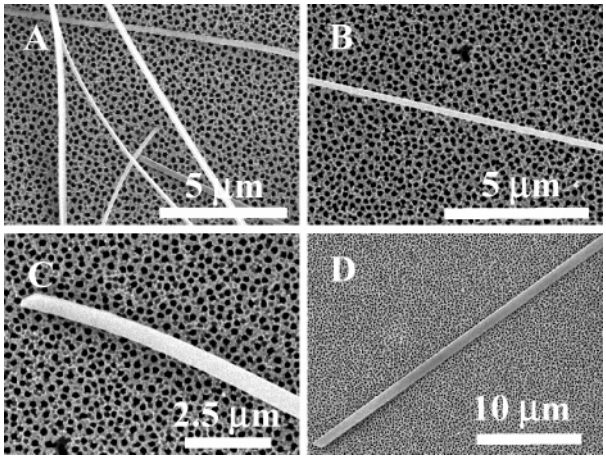

Figure 1. SEM images of F_{16}CuPc submicro- and nanometer-scale ribbons synthesized by the physical vapor transport technique.

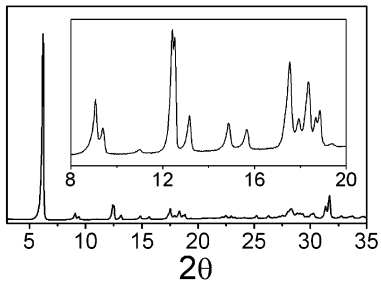

Figure 2. Powder XRD of submicro- and nanometer-scale ribbons of F_{16}CuPc. The inset shows the enlarged part of the XRD spectrum ranging from 8° to 20°.

Results and Discussion

Submicro- and nanometer-scale ribbons of F_{16}CuPc grown on porous alumina membranes are shown in Figure 1. The width of the ribbons ranged from several tens to several hundreds of nanometers, and their length was in the range of several to several tens of micrometers. The size of the products depended on the deposition temperature where porous alumina membranes were located and the deposition time of the physical evaporation. Hence, it is possible to adjust the width of the F_{16}CuPc ribbons from the nanometer to the submicrometer scale by simply controlling the deposition temperature and time of the physical transport process.

Shown in Figure 2 is the X-ray powder diffraction pattern of the submicro- and nanometer ribbons. Thirteen peaks in the lower angle part (less than 20° in 2θ) were used in indexing with the program Dicvol91 (for the indexing result of the powder diffraction pattern, see the Supporting Information, p 1).[9a] Two monoclinic unit cells were proposed by the program. One of them, the lattice parameters of which are $a = 28.33(2)$ Å, $b = 4.755(6)$ Å, $c = 10.17(1)$ Å, and $\beta = 93.17(8)°$, is thought to

(4) (a) Duan, X.; Huang, Y.; Cui, Y.; Wang, J.; Lieber, C. M. *Nature (London)* **2001**, *409*, 66−69. (b) Huang, Y.; Duan, X.; Wei, Q.; Lieber, C. M. *Science* **2001**, *291*, 630−633. (c) Huang, Y.; Duan, X.; Cui, Y.; Lauhon, L.; Kim, K.; Lieber, C. M. *Science* **2001**, 294, 1313−1317.
(5) (a) Bao, Z.; Lovinger, A. J.; Brown, J. *J. Am. Chem. Soc.* **1998**, *120*, 207−208. (b) de Oteyza, D. G.; Barrena, E.; Ossó, J. O.; Dosch, H.; Meyer, S.; Pflaum, J. *Appl. Phys. Lett.* **2005**, *87*, 183504. (c) Sakamoto, Y.; Suzuki, T.; Kobayashi, M.; Gao, Y.; Fukai, Y.; Inoue, Y.; Sato, F.; Tokito, S. *J. Am. Chem. Soc.* **2004**, *126*, 8138−8140.
(6) Zhang, J.; Wang, J.; Wang, H.; Yan, D. *Appl. Phys. Lett.* **2004**, *84*, 142−144.
(7) Laudise, R. A.; Kloc, C.; Simpkins, P. G.; Siegrist, T. *J. Cryst. Growth* **1998**, *187*, 449−454.
(8) Tang, Q.; Li, H.; He, M.; Hu, W.; Liu, C.; Chen, K.; Wang, C.; Liu, Y.; Zhu, D. *Adv. Mater.* **2006**, *18*, 65−68.
(9) (a) Boultif, A.; Louer, D. *J. Appl. Crystallogr.* **1991**, *24*, 987−993. (b) De Wolff, P. M. *J. Appl. Crystallogr.* **1968**, *1*, 108−113. (c) Smith, G.; Snyder, R. *J. Appl. Crystallogr.* **1979**, *12*, 60−65. (d) Ossó, O. *Growth, Structure, and Optical Properties of Highly Ordered Organic Thin Films of Phthalocyanine and Diindenoperylene*; 2004.

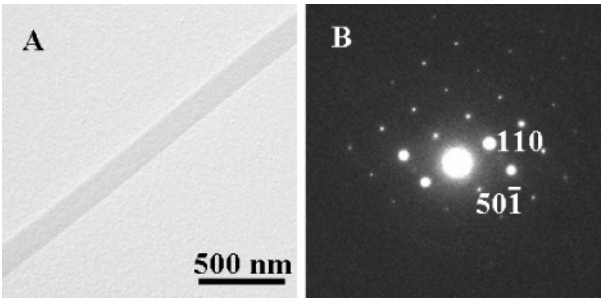

Figure 3. (A) TEM image of an individual nanoribbon of F_{16}CuPc and (B) the corresponding SAED pattern of the nanoribbon.

be more reasonable than the other because, on one hand, it has higher figures of merit ($M(13) = 23.9$, $F(13) = 45.8$)[9b−d] and, on the other hand, lattice constant b agrees very well with the corresponding values in H_2Pc ($b = 4.731$ Å[10]) and β-CuPc ($b = 4.79$ Å[11]). In both H_2Pc and β-CuPc, the molecules are stacked into columns along the b axis through strong $\pi-\pi$ interaction and the dimension of b is actually the distance between two adjacent molecules in the column. Because of the similarity in molecular structure and lattice parameter b, it has been assumed[5a,6] that F_{16}CuPc molecules are also stacked along the b axis to form molecular columns. Unlike b, the lattice parameters a, c, and β are determined by the assembly of molecular columns. Clearly, the peripheral atoms of the molecule will play a dominating role in the assembly of molecular columns since adjacent columns are connected through peripheral atoms. Different from hydrogen, fluorine is the most electron negative element, so peripheral atoms of the F_{16}CuPc molecule are negatively charged, leading to strong repulsion interaction between F_{16}CuPc molecular columns. This may explain why H_2Pc and β-CuPc have similar lattice parameters a, c, and β but the corresponding values of F_{16}CuPc are totally different.

TEM was used to characterize the F_{16}CuPc ribbons. Identical patterns were observed for the different parts of the same ribbon, indicating that the whole ribbon was a single crystal. Several electron diffraction patterns of different zones are observed. All of them could be indexed quite well with the lattice parameters obtained from XRD data. Interestingly, F_{16}CuPc ribbons did not grow along the b axis. As shown in Figure 3, the growth direction of the ribbon was neither parallel with nor perpendicular to any reciprocal lattice vector. It was probably due to the strong negatively charged peripheral atoms of F_{16}CuPc, leading to strong repulsion interaction between F_{16}CuPc molecular columns as mentioned above.

Currently, there are mainly two approaches for the fabrication of single-crystal devices, "electrostatic bonding" [2c,12] and "direct" device fabrication.[2d,e,13] In both cases single crystals are needed to be handpicked and then made into an individual device. The handpicking process limits the work to only rather big crystals, one can hardly imagine the fabrication of devices with very small organic crystals, e.g., submicro- and nanometer-scale ribbons in the present study, by the handpicking process. Moreover, the handpicking process has difficulties with the fabrication of large-area large-scale devices.

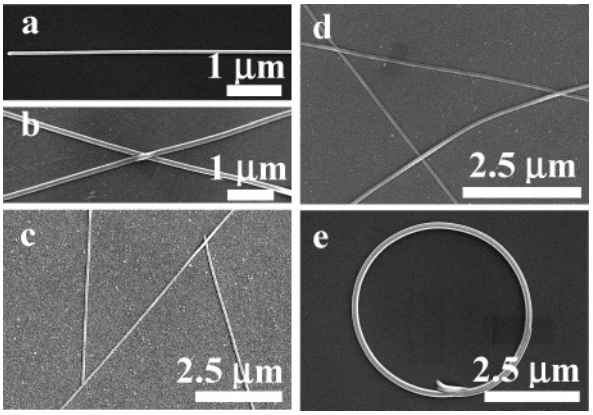

Figure 4. (a) An individual nanoribbon of F_{16}CuPc grown on a SiO_2 surface and (b) cross, (c) "N"-like, (d) "triangle"-like, and (e) "O"-ring-like nanoribbons grown on a SiO_2 surface.

To simplify the device fabrication process and obtain high performance devices, it is desired to grow organic single crystals on the gate insulator directly. Moreover, if the contact between the crystal and the insulator is intimate enough, the crystal/insulator interface will have no chance to be polluted or damaged, leading to much improved device performance and a high yield of device fabrication. We have demonstrated that our CuPc nanoribbons can grow along the surface of the SiO_2, and the devices based on these nanoribbons have a high performance and a high success ratio of device fabrication.[14]

The submicro- and nanometer-scale ribbons of F_{16}CuPc could be in situ grown on a SiO_2 surface. First, previously prepared F_{16}CuPc single-crystalline submicroribbons were put into ethanol and sonicated to get a F_{16}CuPc nanocrystal suspension. Then, Si/SiO_2 substrates, cleaned by organic solvents and oxygen plasma in advance, were dipped into the suspension to predeposit F_{16}CuPc nanocrystals on them. Afterward, the predeposited Si/SiO_2 substrates were transferred into the physical vapor transport system to grow F_{16}CuPc ribbons. It was interesting that F_{16}CuPc submicro- and nanoribbons as well as some well-defined architecture indeed grew along the SiO_2 surface of the substrate, as illustrated in Figure 4a−d. These ribbons can be used to fabricate single-crystal nanodevices directly or in nanodevice coupling for a miniature integrated circuit.

It should be mentioned that these submicro- and nanometer-scale ribbons of F_{16}CuPc possess excellent flexibility. Like our previously reported CuPc submicroribbons,[8] when the submicro- and nanometer-scale ribbons of F_{16}CuPc were manipulated with a mechanical probe under an optical microscope, it was found that the ribbons did not fracture even when they were bent over 360°. Actually, nanoribbons bent like "O" rings were also found in the original products (Figure 4e).

In most cases for the fabrication of OFETs, only one kind of metal, such as Au or Ag, is used as the source and drain electrodes. However, we are not sure such a symmetrical electrode configuration is optimum for the fabrication of our devices, i.e., the devices of F_{16}CuPc submicro- and nanoribbons.

(10) Matsumoto, S.; Matsuhama, K.; Mizuguchi, J. *Acta Crystallogr., C* **1999**, *55*, 131−133.
(11) Brown, C. J. *J. Chem. Soc. A* **1968**, 2488−2493.
(12) (a) de Boer, R. W. I.; Klapwijk, T. M.; Morpurgo, A. F. *Appl. Phys. Lett.* **2003**, *83*, 4345−4347. (b) Mas-Torrent, M.; Durkut, M.; Hadley, P.; Ribas, X.; Rovira, C. *J. Am. Chem. Soc.* **2004**, *126*, 984−985. (c) Podzorov, V.; Menard, E.; Borissov, A.; Kiryukhin, V.; Rogers, J. A.; Gershenson, M. E. *Phys. Rev. Lett.* **2004**, *93*, 086602.
(13) Moon, H.; Zeis, R.; Borkent, E. J.; Besnard, C.; Lovinger. A. J.; Siegrist, T.; Kloc, C.; Bao, Z. *J. Am. Chem. Soc.* **2004**, *126*, 15322−15323.
(14) Tang, Q.; Li, H.; Song, Y.; Xu, W.; Hu, W.; Jiang, L.; Liu, Y.; Wang X.; Zhu, D. *Adv. Mater.*, in press.

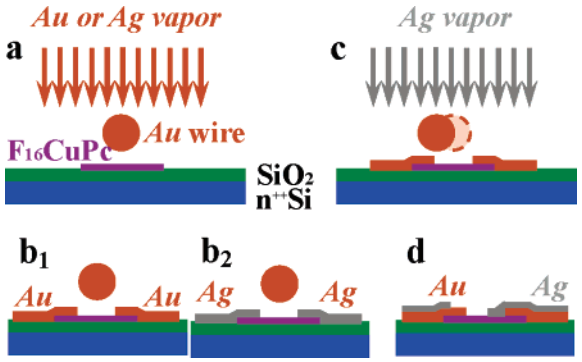

Figure 5. Schematic diagram of the fabrication of OFETs from an individual submicro- or nanometer-scale single-crystalline ribbon of F_{16}-CuPc on Si/SiO_2 (300 nm) substrates. (a, b) Au or Ag gap electrodes were fabricated by thermal evaporation with a micro Au wire as the mask. (c, d) By slightly moving the Au wire mask, Au/Ag gap electrodes were deposited by thermal evaporation.

Usually, in a device the energy level alignment is one of the most important reasons to get efficient carrier injection. Hence, here three kinds of device configurations were used to fabricate our OFETs based on an individual submicro- or nanometer-scale ribbon of F_{16}CuPc. The drain/source electrodes of OFETs consisted of Au/Au, Au/Ag, and Ag/Ag.

Devices based on single-crystal F_{16}CuPc submicro- and nanoribbons were fabricated with a coplanar electrode geometry. The schematic diagram of the device fabrication is given in Figure 5. First, an individual F_{16}CuPc ribbon was in situ grown on the Si/SiO_2 substrate or transferred onto the Si/SiO_2 (300 nm) substrate by mechanical probes.[8] Second, with a micro Au wire as the mask, the Au electrode was deposited onto the substrate by thermal evaporation (as shown in Figure 5a,b). Finally, by slightly moving the Au wire mask, the Ag electrode was fabricated by thermal evaporation, and a gap of several to tens of micrometers was produced between the two electrodes (as shown in Figure 5c,d). Using this method, OFETs with Au/Au, Au/Ag, and Ag/Ag drain/source electrodes could be fabricated. To avoid contamination of the channel surface by metallic atoms deposited at oblique angles under the mask, a homemade "collimator" (a narrow (1 cm i.d.) and long (15 cm) square tube) was used and positioned close to the crystal surface so that the scattering of metallic atoms from residual gas molecules could be cut off from the channel.[2e] Moreover, it is believed that the thermal load on the crystal surface in the deposition process generates traps at the metal/organic interface that results in a poor FET performance.[2d] To minimize the influence of heat (radiation), a small (0.4 mm in diameter) and short (25 mm in length) tungsten wire was used as the thermal evaporation boat, the distance between the thermal evaporation boat and the sample was increased to 35 cm, and the deposition rate was controlled at around 0.2 Å s^{-1}.

In all devices, i.e., devices with Au/Au, Au/Ag, and Ag/Ag drain/source electrodes as shown in Figure 5b,d, n-type transistor behaviors were observed. However, the performance of OFETs with the Au/Ag device configuration exhibited the best behavior (the current and switch-on voltage of devices with Au/Au and Ag/Ag configurations were much worse than those of devices with the Au/Ag configuration as shown in the Supporting Information, p 2). Typical output and transfer characteristics of OFETs based on an individual submicrometer/nanometer ribbon of F_{16}CuPc with the Au/Ag configuration are shown in

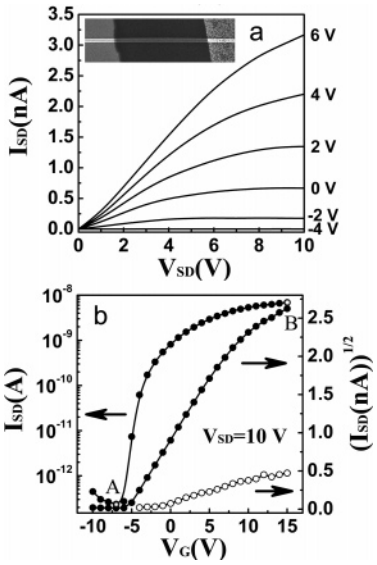

Figure 6. (a) Output characteristics of the device using Au/Ag as the drain/source electrodes. The inset shows the SEM image of the device based on an individual F_{16}CuPc single-crystal submicroribbon. The channel length is ~10 μm, and the width is ~350 nm (width of the ribbon). All measurements were performed in air at room temperature in the dark. (b) Transfer characteristics of the OFET at a fixed source/drain voltage, V_{SD} = 10 V, using Au/Ag (solid circles, positive bias on Au) and Ag/Au (hollow circles, positive bias on Ag) as the drain/source electrodes.

Figure 6. The inset of Figure 6a is the SEM image of an actual device. Although a clear saturation of I_{SD} was observed in Figure 6a, the onset of the curves exhibited nonlinear characteristics, unlike those generally observed in OFETs. Such nonlinear characteristics were also observed by other researchers,[13,15] which could be ascribed to the following: (1) The particular geometry of our device,[15a] where the source and drain contacts were deposited on top of the crystal. Substantial losses were experienced by the drain current when passing twice through the thickness of the crystal, from the source to the channel and back from the channel to the drain electrode. (2) Nonohmic contacts between the drain/source electrodes and the organic crystal. Schoonveld,[15b] de Boer, and Morpurgo et al.[15c] observed such nonohmic behavior of the gold source and drain contacts to the organic active layer (or crystals), even though the work function of gold was ideally aligned to the highest occupied molecular orbital (HOMO) of the molecules. (3) Transformation of carrier injection from Ohm's law to space charge limited current injection due to the influence of traps in the crystal or in the interface of the crystal/insulator.[2e,15d] According to the transfer characteristics, the field-effect mobility (μ), the on/off ratio, the threshold voltage (V_T), and the subthreshold slope (S) of OFETs were calculated at around 0.2 cm^2 V^{-1} s^{-1}, >6 × 10^4 (measured between points A and B as shown in Figure 6b), ~−5.5 V, and 1.1 V/decade, respectively. The performances of the transistors were very stable and highly reproducible in air. To our knowledge, this is the highest mobility for F_{16}CuPc

(15) (a) Horowitz, G.; Garnier, F.; Yassar, A.; Hujhoui, R.; Kouki, F. *Adv. Mater.* **1996**, *8*, 52−54. (b) Schoonveld, W. A.; Wildeman, J.; Fichou, D.; Bobbertk, P. A.; van Wees, B. J.; Klapwijk, T. M. *Nature (London)* **2000**, *404*, 977−980. (c) de Boer, R. W. I.; Stassen, A. F.; Craciun, M. F.; Mulder, C. L.; Molinari, A.; Rogge, S.; Morpurgo, A. F. *Appl. Phys. Lett.* **2005**, *86*, 262109. (d) Lampert, M. A.; Mark, P. *Current injection in solids*; Academic Press: New York and London, 1970; Part 1.

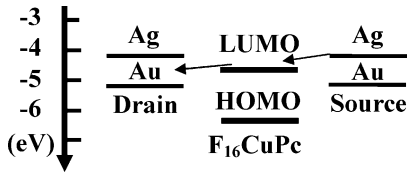

Figure 7. Energy level diagram between $F_{16}CuPc$ and Au and Ag electrodes.

FETs reported to date and is in a class with the highest mobility for air-stable n-type OFETs reported so far.[16]

The high performance of devices with the Au/Ag configuration demonstrated that this kind of device structure was beneficial for charge injection. This is clearly illustrated in Figure 7. For simplicity, the energy levels were drawn as straight lines. The work functions of Au and Ag were assumed as 5.2 and 4.2 eV, respectively. The LUMO level of $F_{16}CuPc$ was addressed around 4.8−4.9 eV.[17] It was obvious that the LUMO level of $F_{16}CuPc$ was lower than the work function of Au and higher than that of Ag to form a stepwise energy level (Figure 7). The stepwise energy level structure avoided the energy barrier between the electrodes and semiconductors and hence effectively facilitated charge injection. Oppositely, if both the source and drain electrodes were Au or Ag, the energy barrier between the LUMO of $F_{16}CuPc$ and the electrodes blocked the electron injection or transport. Furthermore, when the drain/source of devices with the Au/Ag configuration was reversibly biased, i.e., Ag and Au were used as the drain and source electrodes, the performance of the devices was even worse than that of the Au/Au devices due to the double energy barriers for electron injection and transport (shown in Figure 6b by the hollow circles), which confirmed that the stepwise, especially down stepwise, energy level structure of devices with the asymmetrical configuration was effective in improving the device performance.

A series of OFETs were fabricated based on single-crystal submicro- or nanometer ribbons with widths ranging from several tens to several hundreds of nanometers. It was found that the performance of the devices with small channel widths (several tens of nanometers) deteriorated easily in air, although it could gradually recover in a vacuum. However, the performances of the devices with channel widths of hundreds of nanometers were air stable and reproducible. This result probably indicates that the kinetic barrier to moisture and oxygen provided by close-packed fluorine atoms[5] of $F_{16}CuPc$ should not only exist at the surface of the single crystals but also have a penetration depth in the single crystal. Therefore, for devices based on nanoribbons with a width of tens of nanometers, the effective n-type conduction channel width will be remarkably decreased, resulting in the significant influence of oxygen and moisture on their performance. However, for devices based on a single crystal with a width of hundreds of nanometers, the single crystal is big enough that the influence of the barrier layer can be ignored.

In general, single-crystal devices have a lower on/off ratio than thin-film devices, for example, 10^4 vs 10^6 for α-6T,[18] 10^4 vs 10^5 for CuPc,[19] and 10^6 vs 10^8 for pentacene[20] in single-crystal and thin-film transistors, respectively. This probably originates from the disorder and grain boundary defects in the thin-film devices (compared with the single-crystal devices), which will block the carrier transport and hence lead to a lower "off"-state current in the thin-film devices. In the "on" state, the carrier concentration is so high that the disorder and grain boundary hardly affect the on-state current. As a result, the on/off ratio will be higher in the thin-film devices than in the single-crystal devices. However, in our experiment, the on/off ratio of the device based on a single-crystal $F_{16}CuPc$ nanoribbon is over 6×10^4, which is as high as that of the thin-film devices,[5a] indicating that our OFETs based on a single-crystal $F_{16}CuPc$ nanoribbon possess a fairly high performance. This mainly benefits from the excellent stability and electrical characteristics of $F_{16}CuPc$, which ensure that the devices based on $F_{16}CuPc$ nanoribbons can work in a higher current. According to the channel width (300−400 nm, with a height of about 200 nm) and on-state current ($\sim 10^{-8}$ A), the calculated current density across the section of the single crystal (assuming current transported through the whole cross section of the crystal) is over 10 A cm^{-2}, which is so large that most of the organic semiconductors cannot endure. This result shows the excellent stability and electrical characteristics of $F_{16}CuPc$.

Moreover, our OFETs based on $F_{16}CuPc$ submicro- and nanometer-scale ribbons exhibited a subthreshold swing (S) of 1.1 V/decade, which was equivalent to a normalized subthreshold swing (S_i)[2e] of 11 [(V nF)/decade] cm^{-2}, comparable with those of α-Si:H FETs and CuPc single-crystal FETs (with S_i values of ∼10 and 7 [(Vn F)/decade] cm^{-2}, respectively).[19b,21] The small subthreshold slope S_i in our single-crystalline devices reflected the high order of $F_{16}CuPc$ molecules at the interface of the $F_{16}CuPc$ crystal and SiO_2 insulator,[2e] which confirmed the high performance of our single-crystalline OFETs of F_{16}-CuPc ribbons. It is expected that the transistor behaviors of F_{16}-CuPc single-crystalline ribbons will be further improved by the optimization of device fabrication and measurement. First, although $F_{16}CuPc$ is air stable, oxygen etc. in air probably more or less have some influence on the properties of the transistors, especially for devices on the nanometer scale as mentioned above. The measurements in a vacuum and at low temperature may be effective in clarifying this. Second, in field-effect transistors the conduction channel exists exactly at the interface between the ribbon of $F_{16}CuPc$ and the SiO_2 gate insulator; therefore, the optimization of the contact can probably further improve the transistor performance. Recent reports suggest that self-assembling a monolayer onto the SiO_2 gate insulator is effective in improving the contact and subsequently increasing

(16) Jones, B. A.; Ahrens, M. J.; Yoon, M.-H.; Facchetti, A.; Marks, T. J.; Wasielewski, M. R. *Angew. Chem., Int. Ed.* **2004**, *43*, 6363−6366.
(17) (a) Knupfer, M.; Peisert, H. *Phys. Status Solidi A* **2004**, *201*, 1055−1074. (b) Ye, R.; Suzuki, K. *Appl. Phys. Lett.* **2005**, *86*, 253505. (c) Shen, C.; Kahn, A. *J. Appl. Phys.* **2001**, *90*, 4549−4554.
(18) (a) Dodabalapur, A.; Torsi, L.; Katz, H. E. *Science* **1995**, *268*, 270−272. (b) Horowitz, G.; Garnier, F.; Yassar, A.; Hajlaoui, R.; Kouki, F. *Adv. Mater.* **1996**, *8*, 52−54.
(19) (a) Bao, Z.; Lovinger, A. J.; Dodabalapur, A. *Appl. Phys. Lett.* **1996**, *69*, 3066−3068. (b) Zeis, R.; Siegrist, T.; Kloc, C. *Appl. Phys. Lett.* **2005**, *86*, 022103.
(20) (a) Lin, Y. Y.; Gundlach, D. J.; Nelson, S. F.; Jackson, T. N. *IEEE Electron Device Lett.* **1997**, *18*, 606−609. (b) Knipp, D.; Street, R. A.; Völkel, A.; Ho, J. *J. Appl. Phys.* **2003**, *93*, 347−355. (c) Butko, V. Y.; Chi, X.; Lang, D. V.; Ramirez, A. P. *Appl. Phys. Lett.* **2003**, *83*, 4773−4775.
(21) Kanicki, J.; Libsch, F. R.; Griffith, J.; Polastre, R. *J. Appl. Phys.* **1991**, *69*, 2339−2345.

the field-effect mobility of organic transistors.[22] Such an investigation for our F_{16}CuPc ribbon devices is now under way.

Conclusion

(1) Single-crystalline submicro- and nanometer-scale ribbons of F_{16}CuPc were synthesized by a physical vapor transport technique, and their structure has been determined. (2) The submicro- and nanoribbons could be in situ grown along the surface of SiO_2 during synthesis. The "in situ growing process" is free from the general disadvantages of the handpicking process for the fabrication of organic single-crystal devices, such as surface contamination and crystal damage. Moreover, this technique provides a chance to construct architectures of nanometer-scale organic single crystals. (3) Asymmetrical drain/source (Au/Ag) electrodes were introduced into OFET fabrication. High performance was observed in these devices. The field-effect mobility was over 0.2 $cm^2\ V^{-1}\ s^{-1}$ with the on/off ratio at over 6×10^4. The performances were much better than those of devices with symmetrical drain/source electrodes (Au/Au or Ag/Ag). This could be explained by the asymmetrical drain/source electrode configuration, which resulted in the building of a stepwise energy level between the electrodes and the lowest unoccupied molecular orbital of F_{16}CuPc, benefiting electron injection and transport. (4) The performances of the transistors were air stable and highly reproducible.

Acknowledgment. We are grateful to Prof. Daoben Zhu and Prof. Yunqi Liu (Institute of Chemistry, Chinese Academy of Sciences), Prof. Chunli Bai (Chinese Academy of Sciences), Prof. Chen Wang (National Center for Nanoscience and Technology), Dr. Meng He (National Center for Nanoscience and Technology), Dr. Oriol Ossó (Universitat Autònoma de Barcelona), and Dr. Esther Barrena (Max-Planck-Institut für Metallforschung) for profound discussions. We acknowledge financial support from the National Natural Science Foundation of China (Grants 20421101, 20404013, 20402015, 20571079, 20527001, 90401026, 20472089, and 90206049), Ministry of Science and Technology of China (973 Program, No. 2006CB80-6200), Chinese Academy of Sciences, and National Center for Nanoscience and Technology. This paper is dedicated to the Institute of Chemistry, Chinese Academy of Sciences, on the occasion of its 50th anniversary.

Supporting Information Available: Table indicating indexing results of the powder diffraction pattern and figure showing the current and switch-on voltage of devices with Au/Au and Ag/Ag configurations. This material is available free of charge via the Internet at http://pubs.acs.org.

JA064476F

(22) (a) Kobayashi, S.; Nishikawa, T.; Takenobu, T.; Mori, S.; Shimoda, T.; Mitani, T.; Shimotani, H.; Yoshimoto, N.; Ogawa, S.; Iwasa, Y. *Nat. Mater.* **2004**, *3*, 317−322. (b) Lin, Y.; Gundlach, D.; Nelson, S.; Jackson, T. *IEEE Electron Device Lett.* **1997**, *18*, 606−608. (c) Gundlach, D.; Nichols, J.; Zhou, L.; Jackson, T. *Appl. Phys. Lett.* **2002**, *80*, 2925−2927. (d) Ashkenasy, G.; Cahen, D.; Cohen, R.; Shanzer, A.; Vilan, A. *Acc. Chem. Res.* **2002**, *35*, 121−128. (e) Briseno, A.; Aizenberg, J.; Han, Y.; Penkala, R.; Moon, H.; Lovinger, A.; Kloc C.; Bao, Z. *J. Am. Chem. Soc.* **2005**, *127*, 12164−12165.